sciendo

DOI 10.2478/ama-2023-0058

acta mechanica et automatica, vol.17 no.4 (2023)

EXPERIMENTAL INVESTIGATION OF A UNIAXIAL DIELECTRIC ELASTOMER GENERATOR

Wojciech SIKORA*

*Faculty of Mechanical Engineering and Robotics, Department of Machine Design and Maintenance,
AGH University of Krakow, al. Mickiewicza 30, 30-059 Kraków, Poland

wosikora@agh.edu.pl

received 8 February 2023, revised 29 April 2023, accepted 14 May 2023

Abstract: The widespread use of battery-powered electronic devices creates the need to develop methods to extend their maximum operating time. This can be achieved by using ambient energy, which would otherwise be dissipated. The conversion of energy, usually mechanical energy, into electric energy takes place in energy harvesters. Energy harvester systems based on a dielectric elastomer (DE) are a relatively new field that is being constantly developed. Due to their features, dielectric elastomer generators (DEGs) may complement the currently dominant piezoelectric harvesters. The major feature of employing a hyperelastic material is that it allows relatively large displacements to be utilised for generating energy, which is impossible in the case of piezoceramics. This article presents a DEG designed to operate under uniaxial tensile loads and which has a multilayer structure, describes the general operating principles of a DEG, explains the construction and assembly process of the investigated design and shows the electric circuit necessary to properly direct current flow during the DEG operation. The experimental part consists of two series of tests based on a central composite design (CCD). The objective of the first part was to map a capacitance response surface of the DEG in the selected range of the cyclic mechanical load. The second part concerned the amount of generated energy for the specific load case as a function of operating voltages. The result of the work is the formulation of regression models that allow the characteristics of the presented DEG design to be identified.

Key words: dielectric elastomer, energy harvester, DEG, uniaxial tension

1. INTRODUCTION

The utilisation of ambient energy, by harvesting it using dedicated devices and converting it into electric energy, allows the extension of the operating time of small electronics or even the design of self-powered systems. The use of the energy that would otherwise be dissipated also corresponds to the trend of sustainability and ensures that available resources are used in the best way currently possible.

The most common harvester systems are based on piezoelectricity [1,2] or electromagnetics [3,4]. Another group are dielectric elastomer generators (DEGs), which utilise changing capacitance to convert mechanical energy into electric energy. As piezoelectric devices are a well-known and popular solution for harvesting ambient energy, it is convenient to consider dielectric elastomer (DE) features compared with them. The major characteristic of DE devices is the utilisation of a hyperelastic material with stiffness several orders lower than that of piezoelectric materials (especially ceramics). In combination with the fact that DEGs, for proper operation, usually require quite large deformations, it can be concluded that piezoelectric generators cannot be directly replaced by DEGs, and vice versa. Piezoceramics undergo small strains and are highly vulnerable to tensile loads. Thus, DEGs can fulfil the role of a complementary solution to piezoceramics in the field of energy harvesting.

Similarly to piezoelectric devices, systems utilising DEs can function not only as generators but also as actuators (DEA, dielectric elastomer generator). Design challenges are common for both types of devices, especially regarding assembly, electric breakdown or mechanical stability. DE actuators are an important segment of soft robotics, where they are used in biomimetic robots and manipulators [5,6].

The majority of studies concerning DEGs describe the laboratory tests of various prototypes, with generated energy in the range of micro- or milliwatts [7,8]. Nonetheless, there are a few examples of large-scale projects that provide more power and are mainly designed for the conversion of kinetic energy of sea waves [9,10].

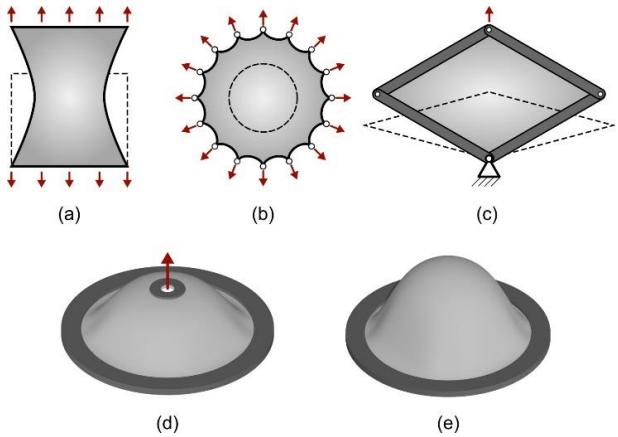

Fig. 1. DEG common types: (a) uniaxial, (b) equibiaxial, (c) diamond, (d) conical, (e) diaphragm

From the mechanical standpoint and based on how they are physically loaded during operation, DEGs can be divided into the following major types [11], as shown in Fig. 1:

DOI 10.2478/ama-2023-0058

- uniaxial,
- equibiaxial,
- diamond,
- conical,
- circular diaphragm.

Each of these designs has benefits and drawbacks, but cone and diaphragm types are most commonly used due to their relatively easy assembly and application. To ensure mechanical stability and avoid buckling during the DEG operation, it is necessary for the elastomer layer to be pretensioned. For a single layer, this is easily achieved in the designs from Fig. 1c–e; it is not required in the equibiaxial variant (Fig. 1b) and is problematic in the case of uniaxial designs (Fig. 1a). For a uniaxial DEG, there is no axial symmetry, especially in a boundary fixture, like in circular designs. Nonetheless, the pretension has to be applied in both axial and transverse directions to maintain the mechanical stability of the layer during cyclic operation.

This article presents an experimental investigation of a DEG operating in a uniaxial mode. It has a multilayer structure with compliant electrodes enclosed between external, elastomer layers. The performed analysis considers a capacitance change and the amount of generated energy of the given DEG design. The observations are further presented in the form of linear regression models, enabling interpolation and, to an extent, extrapolation of the registered data.

2. PRINCIPLE OF OPERATION

The most important trait of a DEG is the requirement to connect it to a DC voltage supply. Initially, this seems counter-intuitive as a DEG aim is to generate electric energy. However, its function does not depend on directly generating potential difference as a response to a physical deformation. A typical elastomer material does not have any inherent piezoelectric properties that would allow such behaviour. Instead, a DEG's actual task is to boost the electric potential of the fixed amount of electric charge.

In general, elastomers are dielectric materials and, therefore, can function as a core material in a plate capacitor. By covering opposite sides of an elastomeric sheet with a conductive layer that performs the role of a compliant electrode, such a capacitor can be created. It is, in fact, a non-polarised variable capacitor as, by applying physical deformation to it, its capacitance will change. This is crucial to the operating principle of DEGs.

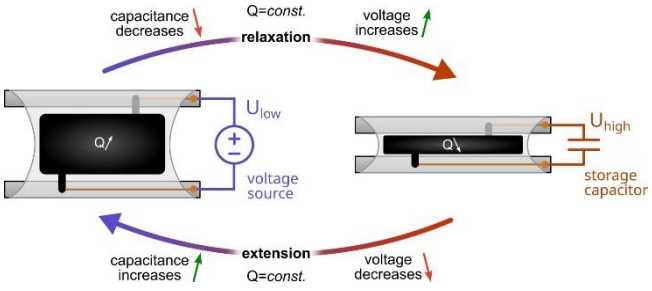

Fig. 2. Operating principle of a uniaxial DEG

Fig. 2 presents the working principle diagram of a DEG based on an elastomer membrane undergoing a uniaxial load. The left side shows a stretched (physically loaded) membrane with a conductive (black) area, which performs the role of an electrode. It also has to be mirrored on the underside of the membrane to obtain the opposite electrode of the same shape and area. At this stage, the DEG has to be connected, through terminals, to a DC supply which provides a constant voltage (U_{low}). This may be a battery or a laboratory supply. Charge flows to the electrodes till the voltage reaches U_{low}. The final amount of accumulated charge is adequate to U_{low} and the actual capacitance of the system. Capacitance is maximum at this stage as the elastomer is deformed and has an increased area. During the transition to the relaxed state (on the right), system capacitance decreases due to membrane area reduction. To ensure that the charge remains constant, the connection with the voltage source U_{low} has to be separated to prevent the charge flowing out. For the separated system to maintain equilibrium, voltage between the electrodes has to increase with decreasing capacitance. This phenomenon occurs due to the conversion of mechanical energy (elastic return of the elastomer) into electric energy (increased potential of the charge), which is caused by mechanical forces overcoming electrostatic forces between elastomeric capacitor electrodes. At that point, to receive the uplifted charge, another circuit has to be connected to the system. This is usually some storage capacitor which has to be already initially charged up to the high voltage U_{high}. It is assumed that the system's voltage after membrane relaxation is $U > U_{high} > U_{low}$. Therefore, the excess charge flows from the system to the storage capacitor, which corresponds to the amount of generated electric energy. After stretching the membrane again, the whole cycle repeats. The DEG function can be best described as similar to that of a "charge pump" that moves the electric charge from U_{low} to U_{high}.

It is important to note that, in an actual system, the periods of charging and discharging the elastomeric capacitor take place not at specific points but during fragments of, appropriately, loading and relaxing half cycles. This will be shown later in Fig. 13 on the registered voltage and charge signals.

3. PREPARATION OF SAMPLES

A thin membrane stretched between two bars subject to a uniaxial load, as a general concept, is often referenced in the literature. However, practical tests of such a DEG are seldom presented. More often DE systems of similar construction, but operating as actuators, can be found [12].

Fig. 3 shows consecutive assembly steps of a DEG. It starts with preparation of a small strip (50 mm × 30 mm × 1 mm) of VHB4910 acrylic foam, which is next stretched ca. 3.6 times in both, perpendicular, directions. As the stretch is applied only along two opposite edges, the silhouette of the expanded layer resembles an hourglass. The first practical problem arises with the practical realisation of a simultaneous expanding layer in two directions. This was performed with the help of a scissor mechanism that can be used for this purpose [13]. The prepared layer was next transferred to the surface of two, parallelly aligned, bars fixed in place at a constant distance of 36 mm from each other. In the physical sample, this constant distance was ensured by two extra L-shaped profiles screwed to the sides of bars, which were removed after the DEG was mounted in the test rig. Excessive parts of the layer were cut (red hatching in Fig. 3). Next, a thin layer of conductive grease (MG Chemicals 846-80G) was applied in the middle and strips of metallic tape that serve as connection terminals were placed. It is crucial that metallic paths have to be

located in the part of the layer that does not deform during operation, otherwise it would lead to an imminent rupture of the layer during operation. The exact same procedure was carried out for the second and the third layers, but in the case of the third one, no conductive grease nor metallic paths were placed. Fig. 3 shows a DEG section of a fully assembled sample.

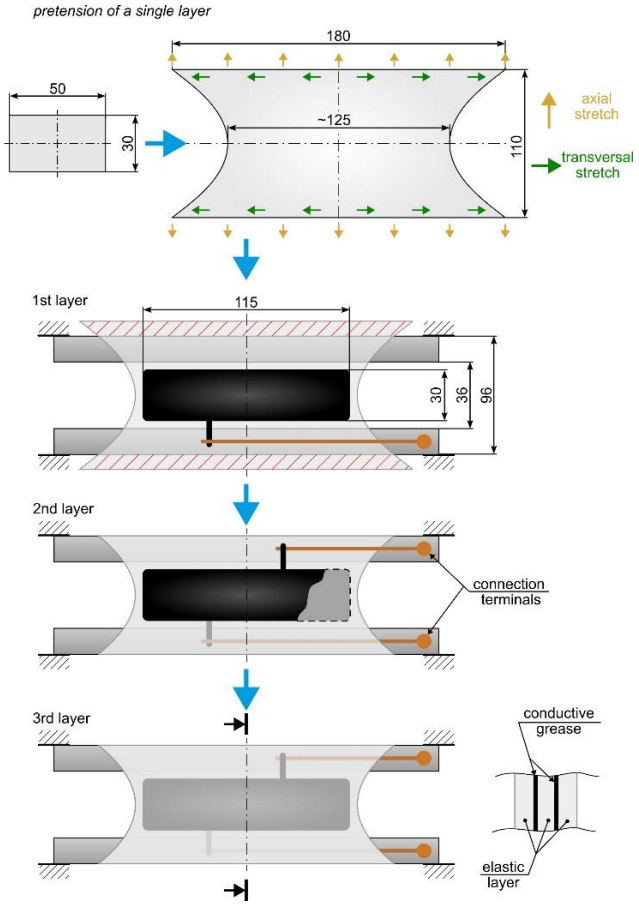

Fig. 3. Assembly stages of the DEG

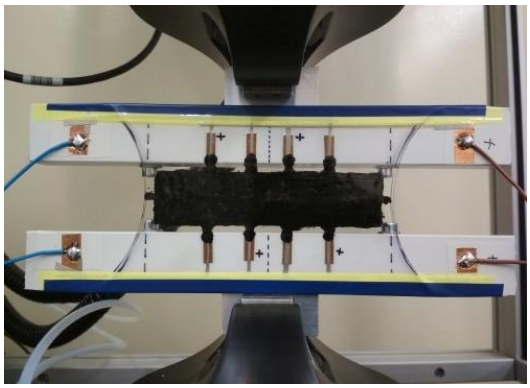

Fig. 4. Mounted DEG sample on the test rig

The conductive layer has significant internal resistance. For a given area of ca. 115×30, resistance measured diagonally is around $20 \div 30\ \mathrm{k\Omega}$. To minimise the distance along the conductive layer that the electric charge has to travel, four, instead of one (in Fig. 3), connections between the metallic paths and the active area were placed for both electrodes. This can be seen in Fig. 4 and it allowed the effective resistance of the conductive layer to be reduced to ca. $5\ \mathrm{k\Omega}$.

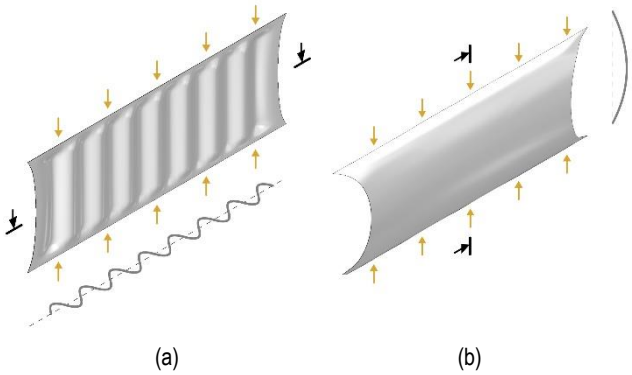

Fig. 5. Possible mechanical instabilities (buckling) appearing in an elastomeric membrane during unloading due to insufficient pretension in the (a) transverse, (b) axial direction

The importance of a preliminary stretch of elastic layers can be illustrated through Fig. 5. Due to the viscoelastic properties of the utilised elastomeric material, during cyclic loading of a sample, in an unloading half-cycle when the displacement speed is too great, the layer can temporarily lose its tension causing mechanical instability. When the relaxation is too fast in the transverse direction, it generates wrinkles similar to those in Fig. 5a; when it happens in the axial direction, the layer forms a bulge (Fig. 5b). While the second case can be easily dealt with by applying higher mean displacement during cyclic loading, the first one can only be diminished through applying the proper transverse pretension of a layer during sample assembly.

The multilayer structure in the presented construction is dictated by improved handling of the sample. Such a DEG could be assembled using only one elastic layer, however, active conductive areas would be exposed and more prone to accidental damage. Moreover, using three layers makes connection of the underside electrode easier. The current design is more durable and simpler to handle. It can also be a foundation for future designs utilising additional electrode layers.

4. ELECTRIC CIRCUIT

The generation of electric energy by a DE undergoing cyclic deformation can be conducted only while properly directing the electric current in the whole system. This can be realised with a dedicated circuit (Fig. 6). In general, the most important elements of the circuit are two diodes (2, 3) that function as check valves and prevent reverse current flow. Operational voltage levels are dictated by the lower voltage source (1) and initially charged storage capacitor (4). The DEG itself is, in fact, a non-polarised variable capacitor (5). Voltage U_{low} (1) can be provided by a laboratory power supply with a step-up converter.

Unlike in a laboratory, in field applications of DEGs, providing a constant supply of voltage in the range of hundreds or thousands of volts as U_{low}, can be a practical obstacle. Therefore, a different solution can be found in the literature, for instance, in Ref [14], a classic circuit is expanded by adding a self-priming circuit. When supplied with a 6 V battery, such circuit can prime up the U_{low} voltage level to a given value before transferring the accumulated electric charge further.

The described circuit (Fig. 6) is well known in the field, yet there are some variations of it. The role of a high voltage source is performed by the capacitor (4). However, it is often replaced by a

DOI 10.2478/ama-2023-0058

series of Zener diodes [15], through which current starts to flow after the DEG voltage reaches its equivalent breakdown voltage. Characteristics of such a design are the fixed value of U_{high} and smoother transition between the stages, as described in Fig. 2.

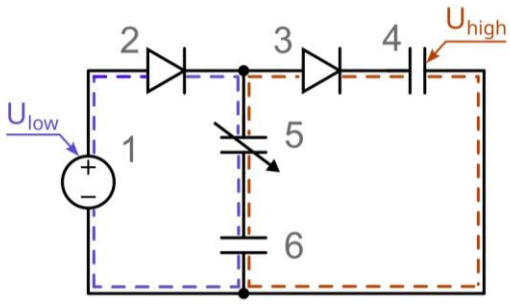

Fig. 6. Electric circuit used for converting energy using a DEG. 1 - low voltage source, 2,3 - diodes, 4 – high-voltage storage capacitor, 5 - variable capacitor (DEG), 6 - capacitor for measuring charge

Another version of the circuit differs by the method of measuring charge flowing in and out of the DEG (5). Here, the measurement is made using an additional capacitor (6) [7] connected in series with the DEG (5). Its capacity (ca. $2.2\ \mu\mathrm{F}$ in this work) should be a few orders higher than that of the DEG (ca. $3.5\ \mathrm{nF}$) so that the voltage drop on it does not significantly affect voltage directly on the DEG. An alternative is to replace the capacitor (6) with a resistor and estimate charge flow through integration of the registered current [15].

As diodes (2, 3) manage the electric current flow, and while charging the DEG, only the left part (violet) of the circuit functions, as shown in Fig. 6,. When the DEG discharges at minimum capacitance, the right part (orange) is active. In between, when the DEG is stretched or relaxed, theoretically, the circuit is inactive as diodes block any current flow. Actually, none of the electronic components are ideal, and leakage currents appear during each of these phases.

5. DESIGN OF EXPERIMENT

The experiment was divided into two parts. One of the major traits influencing the amount of converted energy by the DEG is its capacitance change under a physical load. For the given voltage levels, it determines how much charge can be boosted. Therefore, the first part of the experiment concentrates on the peak-to-peak amplitude ΔC of capacitance during cyclic loading of the sample. Capacitance of the sample was continuously measured using a circuit based on the design described in Ref [16]. The sample was axially loaded with sinusoidally (similar to that in Fig. 7) changing displacement $s(t)$ and at constant frequency f. The remaining parameters, amplitude A and mean displacement m, were changed between test runs. The experiment was performed on an MTS Acumen 3 electrodynamic testing machine.

$$s(t) = m + A \cdot \sin(2\pi f \cdot t) \tag{1}$$

where s is the displacement [mm], m is the mean displacement [mm], A is the amplitude [mm] and $f = 1\ \mathrm{Hz}$ is the frequency.

$$\Delta C = g(m, A) \tag{2}$$

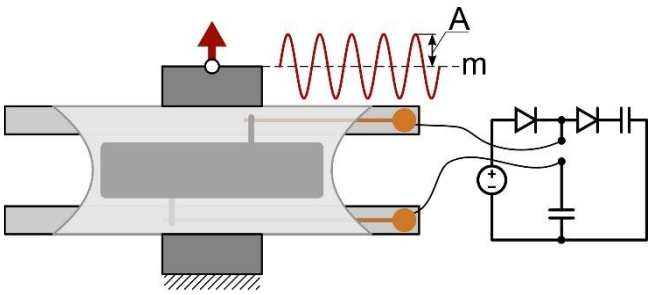

Fig. 7. Sample mounted in the test rig connected with an electric circuit during energy generation measurements

For the sample design and dimensions from Fig. 3, in the course of initial runs, limits of selected factors were determined as follows: amplitude $A = 2 \div 8\ \mathrm{mm}$ and mean displacement $m = -2 \div 2\ \mathrm{mm}$. Too small amplitude can reduce DEG performance to immeasurable levels, while too high amplitude can cause membrane buckling during unloading (as in Fig. 5b). Mean amplitude influences average tension in a membrane as it can encourage buckling if it is too low or, in combination with the amplitude, negatively affects the DEG durability if is too high.

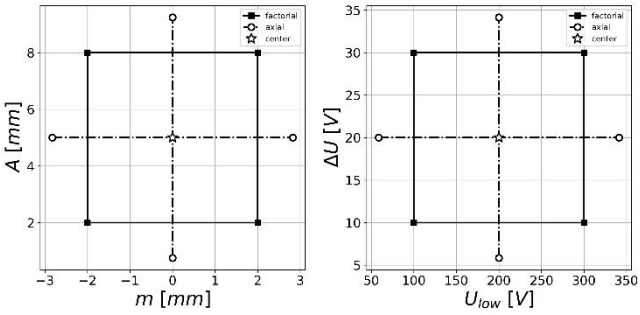

Fig. 8. Design of experiments for investigating (a) capacitance change ΔC (b) generated energy ΔE

These limit values constitute factor points that were next used to plan an experiment based on a central composite design (CCD) [17]. To obtain more general information on the system behaviour, additional points, called central and axial points, were also selected and are presented in Fig. 8a. With three identical samples, three measurements were performed for each of these nine points, giving three replications. Afterwards, the registered data were utilised to fit a linear regression model.

The second part of the experiment was an investigation of the amount of generated energy for the selected point ($A = 8\ \mathrm{mm}$ and $m = 2\ \mathrm{mm}$) from the first part, as a function of U_{low} and ΔU:

$$\Delta U = U_{\mathrm{high}} - U_{\mathrm{low}} \tag{3}$$

$$\Delta E = g(U_{\mathrm{low}}, \Delta U) \tag{4}$$

Apart from the capacitance change, the most important parameters for energy generation in a DEG are voltage levels U_{low} and U_{high}. Lower voltage U_{low} decides on the minimum charge density that is observed in a stretched state (maximum capacitance) of the DEG and, therefore, on the amount of charge that will be later boosted. Instead of directly taking U_{high} into account,

it is more convenient to use the difference ΔU, which determines the level of boost. Extreme values of both U_{low} and U_{high} are limited in theory, from below, by the feasibility of observing phenomena occurring in the DEG, and from the top, by an electric breakdown of the elastomeric layer. Lower voltage levels were assumed as $U_{\mathrm{low}} = 100 \div 300\,\mathrm{V}$ and the difference as $\Delta U = 10 \div 30\,\mathrm{V}$, and these values are presented in Fig. 8b. Similarly to the previous part, a total of 27 test runs were performed, and the results were used to fit a linear regression model.

6. RESULTS AND DISCUSSION

The empirical results acquired during the experiments are grouped in Tabs. 1 and 2. The values are sorted in the following order: rows 1–4 correspond to the factor points, row 5 correspond to the central point, and rows 6–9 correspond to the axial points. Before commencing experiments, there was a doubt concerning whether the manufactured multilayer samples would be identical in terms of their electric properties. Presentation of the data in the form of bar plots shows that in both cases, measured capacitance ΔC (Fig. 9) and generated energy ΔE (Fig. 10) differences between samples are very small. Therefore, measurements performed for each sample can be treated as a replication of the same experimental case. Amplitude and mean value of displacement were converted to strains in Tab. 1, using initial DEG length equal to 36 mm (Fig. 3).

Tab. 1. Capacitance ΔC [nF] measurement results

No.	m [mm]	A [mm]	ε_m [-]	ε_A [-]	Sample 1	Sample 2	Sample 3
1	–2	2	–0.056	0.056	0.56	0.53	0.58
2	–2	8	–0.056	0.222	2.17	2.09	2.14
3	2	2	0.056	0.056	0.62	0.6	0.62
4	2	8	0.056	0.222	2.5	2.32	2.44
5	0	5	0	0.139	1.48	1.4	1.48
6	–2.5	5	–0.07	0.139	1.4	1.31	1.38
7	0	1.2	0	0.033	0.35	0.34	0.35
8	0	8.8	0	0.244	2.55	2.43	2.49
9	2.5	5	0.07	0.139	1.58	1.47	1.38

Tab. 2. Energy ΔE [μJ] measurement results

No.	U_{low} [V]	ΔU [V]	Sample 1	Sample 2	Sample 3
1	100	10	2.39	2.22	2.44
2	100	30	5.46	4.75	5.44
3	300	10	7.65	7.33	7.74
4	300	30	21.25	19.5	21.61
5	200	20	9.48	8.94	9.37
6	73.5	20	2.73	2.51	2.82
7	200	7.4	3.24	3.74	3.93
8	200	32.6	14.55	12.42	14.35
9	326.5	20	16.39	15.68	16.16

The first set of data concerns capacity change as a function of displacement mean and amplitude value. From time series, similar to Fig. 13a, a peak-to-peak amplitude of capacitance ΔC was read. Based on these data and with the help of the Python *Statsmodels* package [18], a regression model was fitted in the following form (capacitance in [nF]):

$$\Delta C(m, A) = 0.0339\, m + 0.2848\, A \tag{5}$$

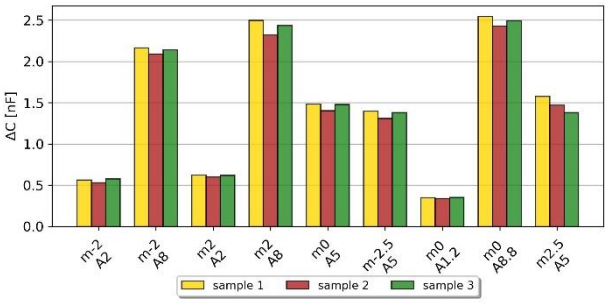

Fig. 9. Comparison of capacitance ΔC experimental results between samples

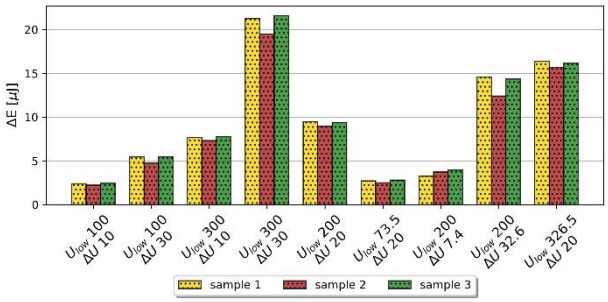

Fig. 10. Comparison of energy ΔE experimental results between samples

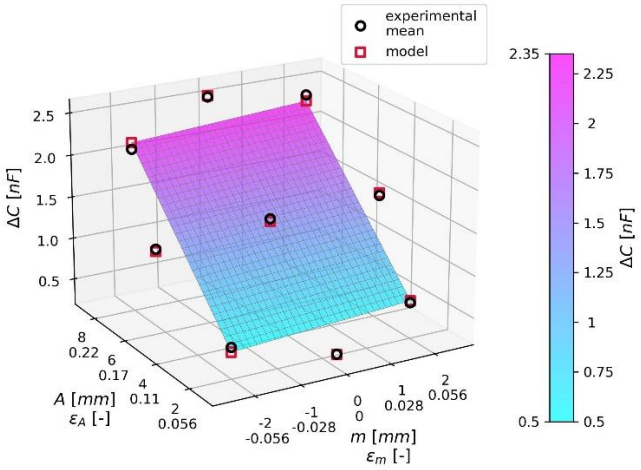

Fig. 11. Comparison of experimental and model results for capacitance change estimation. The surface represents the fitted model within the area designated by the factor points

The obtained coefficient of determination $R^2 = 0.998$ and root mean square error $\mathrm{RMSE} = 0.065$ show that the proposed model very well approximates the ΔC parameter in the investigated range. Visualisation of the data in Fig. 11 contains a comparison between mean experimental values and approximations through the model. Additionally, the response surface corresponding to Eq. (5) for the area designated by four factor points is shown there. The surface is practically flat and inclined only in a single dimension. This implies that mean displacement does not have a significant influence on capacitance change. This is because within the investigated range of m, a significant change in

DOI 10.2478/ama-2023-0058

the transverse dimension of the elastomer layer did not occur. When mean displacement, also in conjunction with amplitude (which would also further imply an interaction effect between these two factors), is large enough, an increase in the DEG area caused by a uniaxial load would be, in part, diminished by a contraction, due to Poisson's effect, in a transverse direction. This can be observed in the so-called strips [19], which are of a slender shape along the load axis. However, this did not occur in the investigated range of load parameters and should be avoided in practice as it lowers DEG performance.

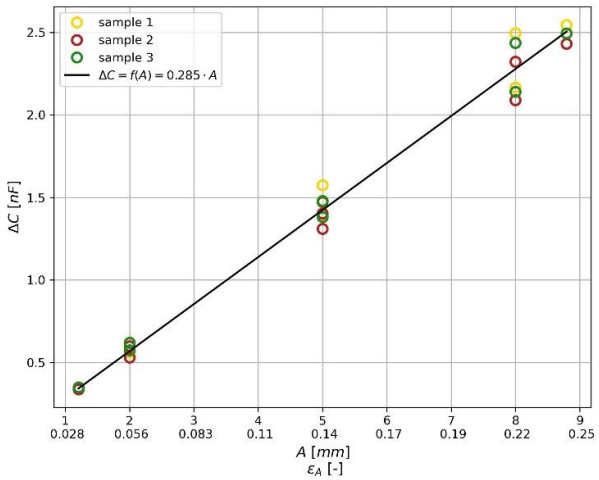

Fig. 12. Comparison between a single-variable regression model and experimental results for capacitance change

Removal of the mean displacement component from Eq. (5) results in a simpler model:

$$\Delta C(A) = 0.2848\, A \tag{6}$$

with a similar value of $R^2 = 0.997$ and comparable $\mathrm{RMSE} = 0.089$. Fig. 12 presents a trend of increasing disparity between the model and experiment with increasing amplitude. This is probably caused by an increasing effect of, omitted here, mean displacement, which, if it has a positive value, can improve minimum tension of the DEG membrane at higher amplitudes. Without the aid of the *m* part at larger amplitudes (>5 mm), the membrane starts to slightly buckle in the relaxation half-cycle, which only slightly affects the effective capacitance change.

The second part of the experiment consists of the measurement of energy generated by the DEG. This was performed for the sinusoidal displacement of $A = 8\,\mathrm{mm}$ and $m = 2\,\mathrm{mm}$. An example of signals registered during measurements, for the central point (Fig. 8b), where $U_{\mathrm{low}} = 200\,\mathrm{V}$ and $\Delta U = 20\,\mathrm{V}$, is presented in Fig. 13. The first plot (Fig. 13a) shows capacitance variability that follows the external physical load in the form of displacement. The second plot (Fig. 13b) is the voltage between positive and negative electrodes of the DEG, which follows stages described in Fig. 2. Fragments where voltage rises or drops are related to relaxation and stretching of the membrane. Boundaries are determined by low and high voltage, and the signal takes a constant value when the DEG is charged or discharged. Fig. 13c, which presents the amount of electric charge accumulated in the DEG, is a kind of negative of Fig. 13b. When voltage is constant, the charge changes, and vice versa. These two signals, voltage and charge in the DEG, are used to estimate energy generated by the DEG.

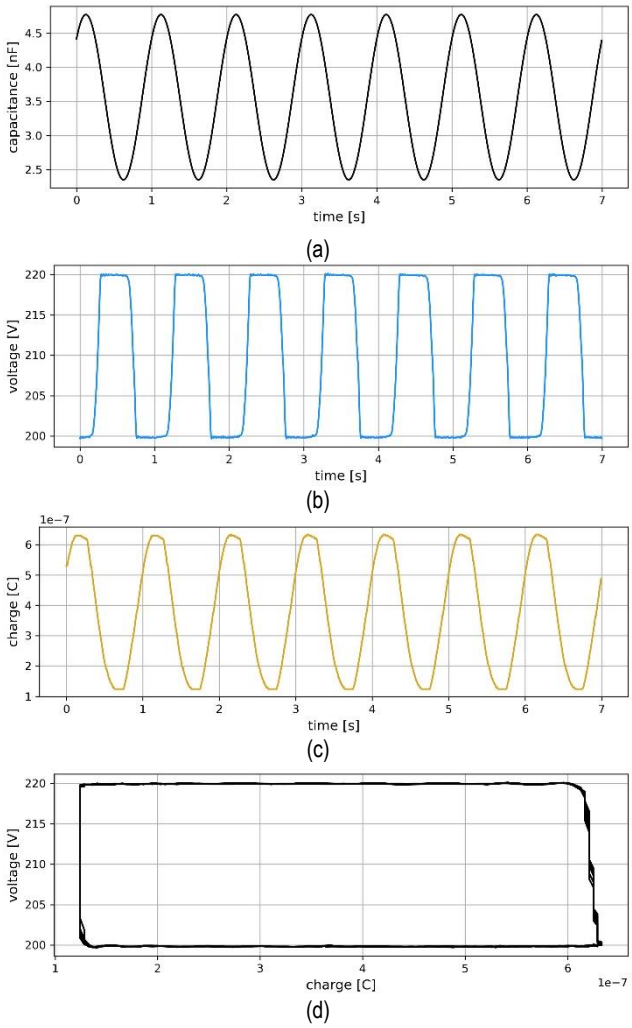

Fig. 13. Signals registered during DEG energy measurement for U_{low} = 200 V and ΔU = 20 V: (a) capacitance, (b) DEG voltage, (c) charge accumulated on the electrodes, (d) U(Q) curve used to estimate energy converted during one full cycle

Fig. 13d sums up the DEG operation and presents voltage as a function of charge. For an ideal system (e.g., in the case of simulation [20]), it should take a rectangular shape. Its area should be equivalent to the amount of energy generated in a single cycle. In the presented case, where curves come from the actual DEG, there are some small leakages, due to which the right side of the rectangle in Fig. 13d is slightly inclined. This can also be seen in Fig. 13c, where charge does not stay perfectly constant at the maximum value. However, in the presented work, it does not significantly influence the amount of generated energy. An example of a similar, but more significant in scale, case can be found in Ref [7], where the mentioned curve has a trapezoidal shape, instead of a rectangular one. Among the sources of such observed behaviour are the diodes (Fig. 6) used in a circuit, through which a very small current flows even when they are in a non-conducting state.

Similarly to the case of measured capacitance, the obtained results of generated energy for the given combinations of U_{low} and ΔU are presented in Fig. 14. The range of generated electric energy is between ca. 2 μJ and 21 μJ, which further equals 2 μW and 21 μW of power as the load frequency was 1 Hz. The relationship between the accounted factors and output energy is more

complex. The regression model based on the experimental data is as follows (energy in [μJ]):

$$\Delta E(U_{\mathrm{low}}, \Delta U) = 0.0045\, U_{\mathrm{low}} + 0.0024\, U_{\mathrm{low}}\Delta U - 0.0774\Delta U \quad (7)$$

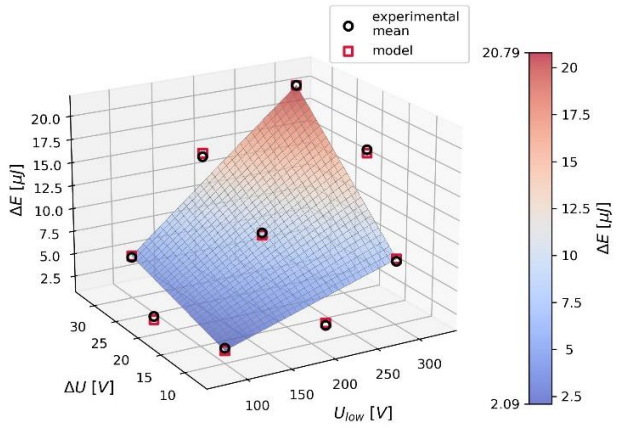

Fig. 14. Comparison of experimental and model results for generated energy estimation. The surface represents the fitted model within the area designated by the factor points

It includes the effects of both factors U_{low} and ΔU and their interaction. The model (Eq. [7]) fits the experimental data very well as it is described by $R^2 = 0.997$ and $\mathrm{RMSE} = 0.597$, as shown in Fig. 14 as a surface plot. Low voltage U_{low} is responsible for the amount of charge accumulated in the DEG at the highest stretch (the highest capacitance); therefore, its significance is clear. The increase in voltage ΔU during DEG relaxation defines how much energy is necessary to boost the deposited charge. An excessively high value of ΔU can result in an interruption of the energy conversion process as the DEG will not be able to boost voltage sufficiently. Thus, no charge flow from the DEG to a storage capacitor will take place. The more the initial charge is deposited as a result of U_{low}, the more energy will be converted at a given level of ΔU, and for that reason, an interaction part was added to Eq. (7).

7. CONCLUSIONS

In the scope of this work, three identical DEG samples were designed and assembled to operate under a uniaxial tensile load. Next, the samples were investigated for capacitance alteration in a given range of physical load parameters. For a selected point from the capacitance experiment, another analysis was performed for the estimation of generated energy. For both cases, linear regression models were fitted to generalise the observations made.

The multilayer structure of the presented DEG allows active layers made of conductive grease to be enclosed between elastomeric layers, improving the handling and durability of the system. The presented design is the final one of several designs considered initially in the course of this work. During the conducted tests, each of the three samples underwent more than 10,000 load cycles without any significant change in their parameters and without any damage to membranes. The high similarity of the obtained results observed between all three samples also shows that using the described design, it is possible to manufacture repeatable samples.

DEGs intended to work in a uniaxial tensile mode are often mentioned in the literature, but examples of working prototypes are sparse. They are often referenced as pure-shear generators [21,22] due to the fact that plane tension can also be interpreted just as pure shear. This is correct, however, under the condition that the membrane width-to-length ratio is >10 and occurring strains are small [23]. In the presented design, this ratio is ca. 3.5; therefore, it should be classified as a uniaxial DEG. The main reason behind utilising wide membranes is to minimise transverse shrinkage during axial extension (Poisson's effect) as it can diminish the capacitance change during loading.

Systems based on DEs can be influenced by a viscoelastic creep [24]. However, in the presented case, registered signals were stable and did not exhibit any long time trends that could be associated with a creep. Most probably it is due to the fact that physical loads during tests were applied with a relatively large rate, that is, a frequency of 1 Hz.

One of the limiting factors in the operation of DEGs is an electrical breakdown of the elastomer membrane. According to Ref [24], a minimum value of electric field that can cause a VHB4910 membrane failure is E≈20 MV/m. This suggests that presented uniaxial DEG was not at risk of breakdown as, in any of tested cases, electric field did not exceed c.a. 2.4 MV/m. DE membrane parameters such as dielectric breakdown strength or electric permittivity can depend on material stretch or temperature [25]. However, working stretches in the performed experiments were relatively small and did not exceed 1.3; therefore, aforementioned effects were not included in the analysis.

Investigation of the capacitance change of the DEG in the selected range of load parameters showed that it is stable and, practically, a linear relation. Mean displacement in $s(t)$ sinusoidal loading has a huge impact on the mechanical stability of the membrane but can be omitted when considering capacitance alone. Initially, there were some doubts whether interaction between layers during cyclic loading can affect DEG parameters as the presence of a conductive grease allows relative slip. However, no such effect was observed in relation to both mean displacement and amplitude. This opens a way to further investigate multilayer structures with additional electrodes.

The amount of energy generated in the researched scope of voltage was between ca. 2 μJ and 21 μJ. Regarding absolute values, it is a small quantity but comparable to those being reported in other works. However, it is worth noting that voltage levels used in the presented DEG are below 350 V, while typical values found in the literature are of a few kilovolts. This is possible due to the quite large capacitance change ΔC that reached almost 2.5 nF.

In the case of both parts of the experiment, linear regression models fitted the empirical data well. Using the further model of Eq. (7) to extrapolate, the presented DEG design has the potential to generate even up to ca. $0.12\, mJ$ if $U_{\mathrm{low}} = 1000$ V and $\Delta U = 50$ V. Increasing frequency over 1 Hz can also increase the amount of generated power.

REFERENCES

1. Grzybek D, Kata D, Sikora W, Sapiński B, Micek P, Pamuła H, Huebner J, Rutkowski P. Piezoelectric particulate composite for energy harvesting from mechanical vibration. Materials. 2020; 21 (13): 1-14. doi: 10.3390/en15176254
2. Micek P, Grzybek D. Impact of a connection structure of Macro Fiber Composite patches on energy storage in piezoelectric energy har-

vesting from a rotating shaft. Energies. 2022; 17 (15): 1-15. doi: 10.3390/en15176254
3. Sapiński B, Jastrzębski Ł, Kozieł A. Ideal Rectifier Bridge Converting the Harvested Energy of Vibrations into Electric Energy to Power an MR Damper. Acta Mechanica et Automatica. 2020; 14 (4): 198 - 205. doi: 10.2478/ama-2020-0028
4. Rosół M, Sapiński B. Ability of Energy Harvesting Mr Damper to Act as a Velocity Sensor in Vibration Control Systems. Acta Mechanica et Automatica. 2019; 13 (2): 135 - 145. doi: 10.2478/ama-2019-0019
5. Liu L, Zhang J, Luo M, Li B, Tang C, Chen H, Yang Z, Li P, Li D. Electro-pneumatic dielectric elastomer actuator incorporating tunable bending stiffness. Physical Review Research. 2020: 2 (2): 023202. doi: 10.1103/PhysRevResearch.2.023202
6. Berlinger F, Duduta M, Gloria H, Clarke D, Nagpal R, Wood R. A Modular Dielectric Elastomer Actuator to Drive Miniature Autonomous Underwater Vehicles. 2018 IEEE International Conference on Robotics and Automation (ICRA). 2018.
7. McKay T, Rosset S, Anderson I, Shea H. Dielectric elastomer generators that stack up. Smart Materials and Structures. 2014; 24: 015014. doi: 10.1088/0964-1726/24/1/015014
8. Zhang C, Lai Z, Zhang G, Yurchenko D. Energy harvesting from a dynamic vibro-impact dielectric elastomer generator subjected to rotational excitations. Nonlinear Dynamics. 2020; 102: 1271–1284. doi: 10.1007/s11071-020-05988-7
9. Moretti G, Malara G, Scialò A, Daniele L, Romolo A, Vertechy R, Fontana M, Arena F. Modelling and field testing of a breakwater-integrated U-OWC wave energy converter with dielectric elastomer generator. Renewable Energy. 2020; (146): 628-642. doi: 10.1016/j.renene.2019.06.077
10. Jean P, Wattez A, Ardoise G, Melis C, van Kessel R, Fourmon A, Barrabino E, Heemskerk J, Queau J. Standing Wave Tube Electro Active Polymer Wave Energy Converter. Proceedings of SPIE - The International Society for Optical Engineering. 2012. doi: 10.1117/12.934222
11. Moretti G, Rosset S, Vertechy R, Anderson I, Fontana M. A Review of Dielectric Elastomer Generator Systems. Advanced Intelligent Systems. 2020;2(10): 2000125. doi: 10.1002/aisy.202000125
12. Goh Y, Akbari S, Vo T, Koh S. Electrically-Induced Actuation of Acrylic-Based Dielectric Elastomers in Excess of 500% Strain. Soft Robotics. 2018; 6 (5): 675-684. doi: 10.1089/soro.2017.0078
13. Araromi O, Gavrilovich I, Shintake J, Rosset S, Shea H. Towards a deployable satellite gripper based on multisegment dielectric elastomer minimum energy structures. Electroactive Polymer Actuators and Devices (EAPAD) 2014. 2014. doi: 10.1117/12.2044667
14. Panigrahi R., Mishra SK. An Electrical Model of a Dielectric Elastomer Generator. IEEE Transactions on Power Electronics. 2018; 33 (4). doi: 10.1109/TPEL.2017.2749329
15. Huang J, Shian S, Suo Z, Clarke D. Maximizing the Energy Density of Dielectric Elastomer Generators Using Equi-Biaxial Loading. Advanced Functional Materials. 2013; 40 (23): 5056-5061. doi: 10.1002/adfm.201300402
16. Gasosoth T, Lianghiranthaworn T, Unai S. A period-based measurement for grounding capacitance meter with Arduino using a relaxation oscillator. Journal of Physics Conference Series. 2020;(1380), doi: 10.1088/1742-6596/1380/1/012074
17. Montgomery DC. Design and Analysis of Experiments. EMEA edition, 9th ed. Hoboken, NJ: John Wiley & Sons; 2017.
18. Seabold S, Perktold J. Statsmodels: Econometric and statistical modeling with Python. Proceedings of the 9th Python in Science Conference. 2010.
19. Lau G, Chen F, Ren Z. Axial force transmission in flexible bowtie dielectric elastomer actuators. Applied Physics Letters. 2022; 120: 012903. doi: 10.1063/5.0072852
20. Sikora W. Adaptation of an energy harvester working in the bending mode to utilize dielectric elastomers. Proceedings of the 22nd International Carpathian Control Conference. 2021. doi: 10.1007/s00707-021-03046-w
21. Chen Y, Kang G, Yuan J, Li T. Experimental study on pure-shear-like cyclic deformation of VHB 4910 dielectric elastomer. Journal of Polymer Research. 2019; 26: 186. doi: 10.1007/s10965-019-1858-6
22. Chen Y, Kang G, Hu Y, Yuan J, Li T., Qu S. Low-cycle electromechanical fatigue of dielectric elastomers: Pure-shear experiments and life-prediction model. International Journal of Fatigue. 2021; 148: 106220. doi: 10.1016/j.ijfatigue.2021.106220
23. Bergström J. Mechanics of solid polymers: theory and computational modeling, San Diego, USA: William Andrew; 2015.
24. Srivastava AK, Basu S. Modelling the performance of devices based on thin dielectric elastomer membranes. Mechanics of Materials. 2019; 137. doi: 10.1016/j.mechmat.2019.103136
25. Khajehsaeid H., Baghshomal Azar H. Influence of stretch and temperature on the energy density of dielectric elastomer generators. Applied Mathematics and Mechanics. 2019; 40: 1547–1560. doi:10.1007/s10483-019-2539-7

This work was supported by the AGH University of Krakow under research program No. 16.16.130.942/B303

Wojciech Sikora: https://orcid.org/0000-0002-2953-5653